HYPERSPECTRAL MEASUREMENTS OF SPACE OBJECTS WITH A SMALL FORMAT SENSOR SYSTEM

Dr. Robert Crow, Dr. Kathy Crow, Dr. Richard Preston
Sensing Strategies, Inc., Pennington, NJ
Dr. Elizabeth Beecher
Air Force Research Lab/RYMT

ABSTRACT

Under an initial study effort for AFRL/RYMT, Sensing Strategies, Inc. is evaluating an inexpensive, very small format proof-of-concept system for collecting spectral data from geosynchronous (GEO) and low earth orbit (LEO) satellites to support space situational awareness (SSA) missions. The system uses a slitless spectrometer and a modified pan/tilt stage for satellite tracking. A goal of the system is to collect signatures with significantly higher spectral resolution than traditional methods that use astronomical filters for multi-spectral measurements. An advantage of this technique is that the spectra are collected simultaneously rather than collecting multi-spectral data sequentially in different bandpasses. The spectral data is being evaluated for its utility to uniquely classify or categorize satellites. This paper will present preliminary measurements of satellites and discuss observations on how the spectral data can improve SSA functions. The approach of using an inexpensive, small format system with no special infrastructure requirements opens the door to collecting satellite reflection measurements from multiple locations simultaneously, which both improves the probability of data collection and provides a richer data set by having concurrent measurements at multiple reflection angles.

1. INTRODUCTION

There have been a number of studies of non-resolved spectral measurements of orbiting debris and man-made objects using meter-class telescopes with grating-based spectrometers to make observations in the visible to 900nm range [1-3]. These large observatory facilities provide a significant light gathering capability for obtaining spectral signatures for smaller space objects, but are obviously not mobile and are expensive and logistically difficult to replicate. A smaller format system that incorporated a diffraction grating into the 16-inch f/8.2 fast-tracking telescope to produce a slitless spectrometer was used to make measurements of two communications satellites in GEO [4]. The study was able to measure a blue-shift in the solar return signature and correlated this to specular glints off of the solar panels around the seasonal equinox. This study showed promise for spectral measurements using a telescope that is smaller than meter-class.

There is a potential benefit of increased spectral resolution for space situational awareness (SSA) missions to monitor man-made satellites. For satellites with known geometric and reflectance properties, the discrimination between different satellites or detection of individual satellite maneuvers can be aided by identifying changes in both overall brightness and spectral profile as different satellite components contribute to the received signature. For unknown satellites, spectral measurements can support the estimation of intrinsic properties of materials used and provide insight as to design and bus type. However, since the observed spectrum for a given satellite is the superposition of the solar reflected signals for all satellite components producing a detectable signature, a small handful of observations alone are not generally sufficient to produce meaningful conclusions. Instead, measurements need to be made over longer periods of time (hours to days depending on the objective) and from multiple locations in order to be able to view a sufficiently dense set of solar reflectance phase angles from each component. In particular for GEO satellites, favorable glint angles that produce specular reflections may occur only seasonally at specific times of day. This motivates the desire for smaller, less expensive spectral sensors that can be widely deployed. Having multiple systems leads to a higher probability of collection in case one site has cloud cover. Using multiple systems also provides data with a diversity of reflection angles. However, this leads to the significant challenge of making observations with very small systems and getting enough signal to produce adequate SNR.

Motivated by the need for spectral data to support SSA and the desire for a system that could be widely deployed, Sensing Strategies has developed a very small format proof-of-concept sensor for collecting spectral signatures of LEO and GEO satellites. The sensor is a slitless spectrometer designed using commercial-off-the-shelf parts in a

custom configuration. The system approach is inexpensive, and a goal is for the system to be deployed and set up quickly without the need for special infrastructure. A novel spectral response calibration technique was developed in a laboratory setting rather than solely relying on stars as calibration sources. The breadboard system was used to collect signatures for several commercial satellites over multiple nights as an initial demonstration of capability. For this paper, a selected data set is processed and analyzed against predicted solar spectral irradiance at the earth's surface. Preliminary observations on the utility of the spectral measurements from the system are discussed.

2. SYSTEM DESCRIPTION

The proof-of-concept system as configured on the tracking mount is shown in Fig. 1. The slitless spectrometer design is relatively simple, consisting of a 6-inch f/9 Ritchey-Chretien telescope (the optical tube on the right side of the photo shown in Fig. 1), a thermoelectrically-cooled CMOS camera, and a transmission grating with good 1st order diffraction efficiency in the visible region. The grating is located just in front of the focal plane of the camera, which in turn is located at the prime focus of the telescope. In addition to the spectrometer, the tracking mount also includes a wide field panchromatic camera (left side of photo in Fig. 1) which is used to support star alignment and tracking functions.

Fig. 1. Photograph of the prototype slitless spectrometer installed on a tracking mount

The slitless spectrometer design produces a field of view of approximately 0.5-degrees square which allows it to measure the entire reflected spectrum from 400 to 850 nm simultaneously. Modifications of the preliminary system parameters are under consideration as requirements for target brightness, time response and spectral analysis are refined. The design allows simultaneous collection of spectra on multiple satellites that fall within the sensor field-of-view. The prototype system leverages satellite tracking capabilities that Sensing Strategies already had in place that provided a good capability to point the spectrometer sensor to desired targets. The system can be set up on a tripod and operated with a laptop computer. Once the system is leveled and the sensors are focused, a star alignment procedure is used to calibrate the pointing of the pan/tilt. The system is able to track both GEO and LEO satellites.

3. CALIBRATION TECHNIQUES

An objective of this effort was to develop a calibration procedure that could be performed in a controlled laboratory setting on the entire sensor optical system, with the eventual goal of producing data products in absolute radiometric units. The small format of our system obviously makes the laboratory calibration objective more feasible as compared to sensors developed around larger telescopes. However, we do envision that ultimately the use of calibration stars would still play a role in characterizing and compensating for atmospheric effects specific to the time and location of a particular satellite reflectance measurement, similar to what has been done in other programs.

Our approach to the laboratory calibration is to produce a calibrated far-field optical source so that spectrometer focus can be maintained in the far field. We also wanted our far-field source to fill the entire spectrometer collection aperture so that the calibration measurements were made using the full f/# of the system; underfilling this aperture would effectively increase the f/# which would artificially reduce any focusing aberrations that are actually present in the system. The calibration approach also needed to allow for different standard sources to be installed into the setup so that both responsivity and wavelength axis (i.e., nm/pixel) could be determined.

Our approach to achieving the far field source is illustrated in Fig. 2, where the calibration source is shown on the left and the spectrometer is shown on the right. For the calibration setup, a slit is placed at the focus of a 10-inch spherical mirror which projects the slit into the far field. An integrating sphere sits just behind the slit to provide a back-illumination which is spatially homogenous, and a calibrated light source is placed at the entrance port of the integrating sphere. The light source can be any standard that is relevant to the calibration, such as a standard lamp or laser. In Fig. 2, the source shown is a spectral calibration lamp which is used to present the spectrometer with a set of known emission lines.

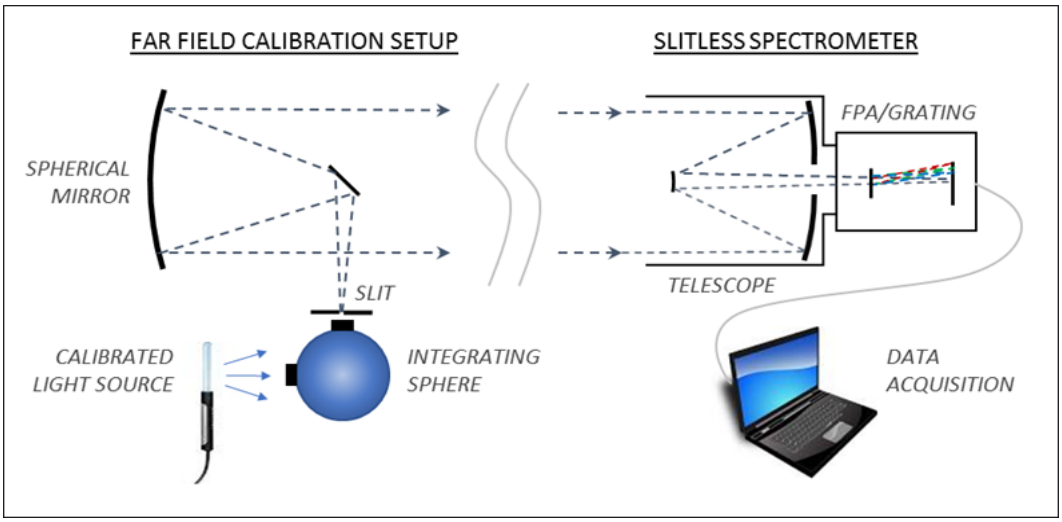

Fig. 2. Schematic of optical calibration setup. The slit aperture in front of the integrating sphere is collimated to produce a far-field source to the spectrometer.

Fig. 3 shows the actual laboratory setup used. On the left, the slitless spectrometer in the foreground is pointed toward the 10-inch collimating mirror in the background. On the right, a calibration lamp is shown next to the integrating sphere, slit, and fold mirror.

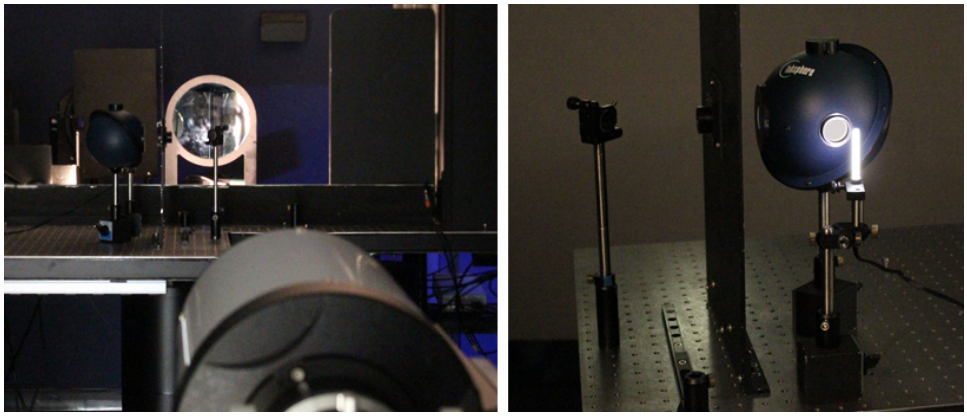

Fig. 3. Elements of the optical calibration setup: the slitless spectrometer and 10-inch collimating mirror (left photo) and the calibration lamp, integrating sphere, the slit (installed in the tall black plate), and fold mirror (right photo).

The calibration source behind the slit produces images with clearly discernable zeroth- and first-order features. For example, Fig. 4 shows a detail view of a spectral image of a krypton line lamp in the calibration setup described above (the image has been contrast-stretched to bring out some of the dimmer features). The zeroth-order feature on the left is an image of the slit aperture itself. The first-order features show replicas of the slit aperture at each of the emission lines of the krypton lamp, where the brightness of each emission line determines the brightness of the feature in the image. A few of the specific line wavelengths are labelled, and these lines can be used to determine or periodically verify the wavelength calibration of the spectrometer. Note also that the width of the slit (the narrowest we had available) spatially overfills multiple pixels, and so this will need to be factored into any evaluation of spectral uncertainty. We have also found that injecting a 632.8 nm helium-neon laser into the integrating sphere is useful to perform a quick check on a single spectral line.

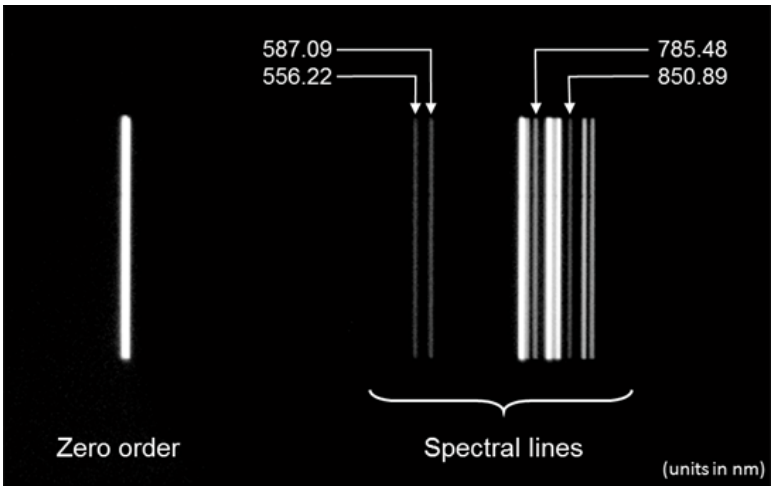

Fig. 4. Slitless spectrometer measurement of a krypton lamp in the far field using the setup shown in Fig. 2. The image shows the zero-order image of the slit (vertical line, left) and the first-order spectral lines (right).

The same setup also allows us to perform broadband radiometric amplitude calibration by replacing the line lamp with a NIST-traceable tungsten lamp which produces a smooth, continuous spectrum that is close in shape to a 3200°K Planck function. This technique is used to produce a known irradiance across all wavelengths, and this is the basis for computing the spectral responsivity which is used to convert digital counts to irradiance units. (In the present effort, we have focused on calibrating to the relative spectral shape with the future goal of producing answers in absolute radiometric units.)

4. FIRST LIGHT DATA SETS

Fig. 5 shows a sub-region of interest from one of the first frames captured with the slitless spectrometer that captured four GEO satellites viewed from Pennington, NJ using a 16 second exposure time. The image is part of a sequence of frames that was captured on 17 May 2017 over the course of nearly six hours. The satellites appear as points of light on the top with their raw vertical spectral signatures appearing as streaks of varying brightness below each point (the image has been contrast-stretched to bring out some of the dimmer features). The specific satellites are Amazonas 2, 3, and 4A on the left and EchoStar 12 on the right. For reference, the separation of the leftmost and rightmost satellites is about 0.25 degrees longitude over the equator. In addition, several stars can be seen as streaks with a slightly negative slope left-to-right, along with their respective spectral signatures descending below the streak. The stars represent clutter which must be mitigated as part of the spectral extraction process.

For this first light data set, the spectral data was reduced using a series of semi-automated steps. A reference pixel for the satellite location was tracked throughout the image sequence based on the zero-order location. This reference pixel then defined a narrow vertical region of interest (ROI) that included all of the energy from the first-order

spectrum. Row sums were performed across this ROI to produce a raw spectral signature vector in camera digital counts. Several background and clutter subtraction steps were then performed to correct for nonuniformity in background and to isolate the signature of the satellite from unwanted contributions from streaking stars. The native spectral resolution based on pixel size is not practical as the SNR is low. Therefore, spectral binning of the signature vector was used to increase the SNR per spectral bin, at the expense of spectral resolution. After some experimentation, we arrived at a spectral bin width which is still much higher in spectral resolution than typical astronomical filter bands (e.g., UVBRI and similar) and provides a well-resolved spectrum from the standpoint of observing changes in spectral shape due to the favorable illumination geometry of different materials on the satellite. Finally, the spectral responsivity correction is applied on a frame-by-frame basis to produce the evolution of the satellite reflectance spectrum over the course of the observation period.

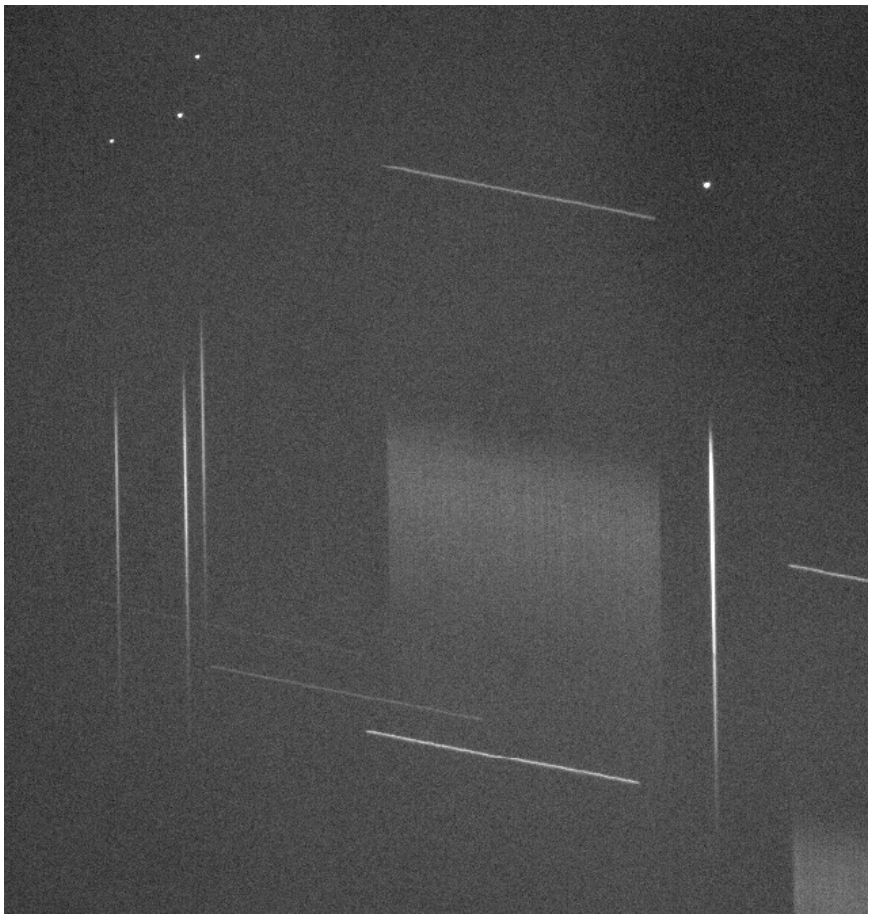

Fig. 5. Sub-region of a single frame from slitless spectrometer showing four GEO satellites (dots and corresponding vertical lines) and several stars (diagonal streaks).

The above procedure was applied to extract the temporal sequence of spectral signatures for EchoStar 12 from the 17 May image sequence. Fig. 6 shows a plot of one of the spectral signatures from the sequence that has been normalized to unity at its maximum and spectrally binned in order to provide signal averaging to improve signal to noise ratio (SNR). This binning is important especially at wavelengths longer than 800 nm as the combination of decreasing camera responsivity and decreasing diffraction efficiency of the grating at these wavelengths leads to greatly reduced responsivity with increasing wavelength. We have found that for the current optical configuration, the SNR becomes poor beyond 850 nm, and therefore we chose to limit the spectral extent to 850 nm.

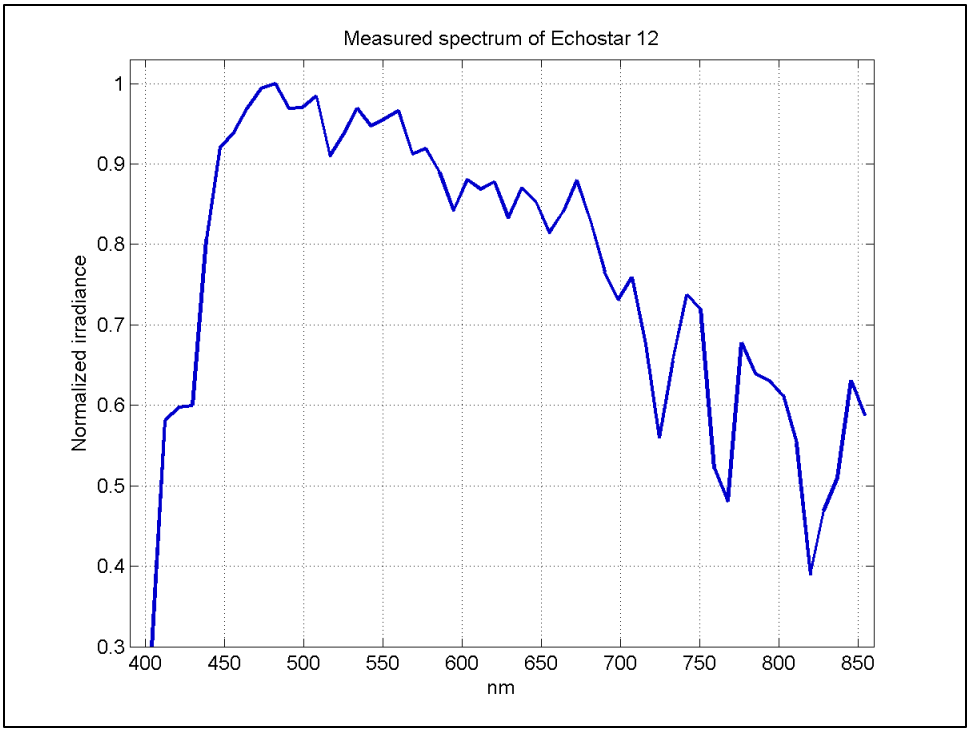

Fig. 6. Measured solar reflectance spectrum from EchoStar 12

There are a number of obvious features in the measured spectrum that appear as peaks and valleys. We wanted to establish a basis for understanding whether these features were real or whether they were system artifacts resulting from the sensor and/or processing procedures. Since the reflectance spectra from satellites in this wavelength region result purely from solar illumination, we decided to compare the measured spectra to solar spectra generated using MODTRAN. Specifically, we wanted to compute the direct solar spectral irradiance on the ground to investigate how the standard atmospheric absorption bands lined up with our data.

Fig. 7 shows the model comparisons to the same spectrum shown in Fig. 6. For the MODTRAN direct solar irradiance calculation, a mid-latitude summer, rural, 23 km visibility atmospheric model was used to approximate our central New Jersey location, and the solar geometry was chosen to be at the same elevation of the satellite. The measured EchoStar 12 spectrum (blue trace) is normalized to match the direct solar spectral irradiance (green trace) at around 450 nm, thus anchoring these spectra together at one wavelength to allow for comparison in spectral shape. The correlation between the measurement and model prediction is immediately evident in the alignment of the H_2O absorption bands around 720 nm and 820 nm and the O_2 absorption band at 760 nm as indicated by the dotted vertical lines on the right side. Another feature indicated by a vertical line is the dip around 430 nm. This corresponds to a Fraunhofer line present in the spectrum of the sun itself as seen in the top-of-the-atmosphere solar spectrum (red trace) which was also generated using MODTRAN.

The ability of the slitless spectrometer to measure each of these absorption lines suggests that the system can resolve changes in spectral features of the satellite reflectance beyond the resolution of standard astronomical filter bands. Furthermore, the possibility exists to utilize the measured atmospheric absorption bands to determine in situ atmospheric transmission over the actual optical path that would be concurrent with the satellite reflectance measurement.

The overall spectral shape of the EchoStar 12 spectrum is clearly blue-shifted relative to the ground-solar spectrum as seen in Fig. 7. This is likely the result of solar panel reflection dominating the total solar reflectance. If the measurement had been made closer to one of the equinoxes, at which time the specular angle from the solar panel would be more favorable, then we would expect to see a brighter signal that is even more blue-shifted. Since our

measurement was made closer to the summer solstice, we are encouraged that the spectrometer has the potential to produce useful data throughout the year.

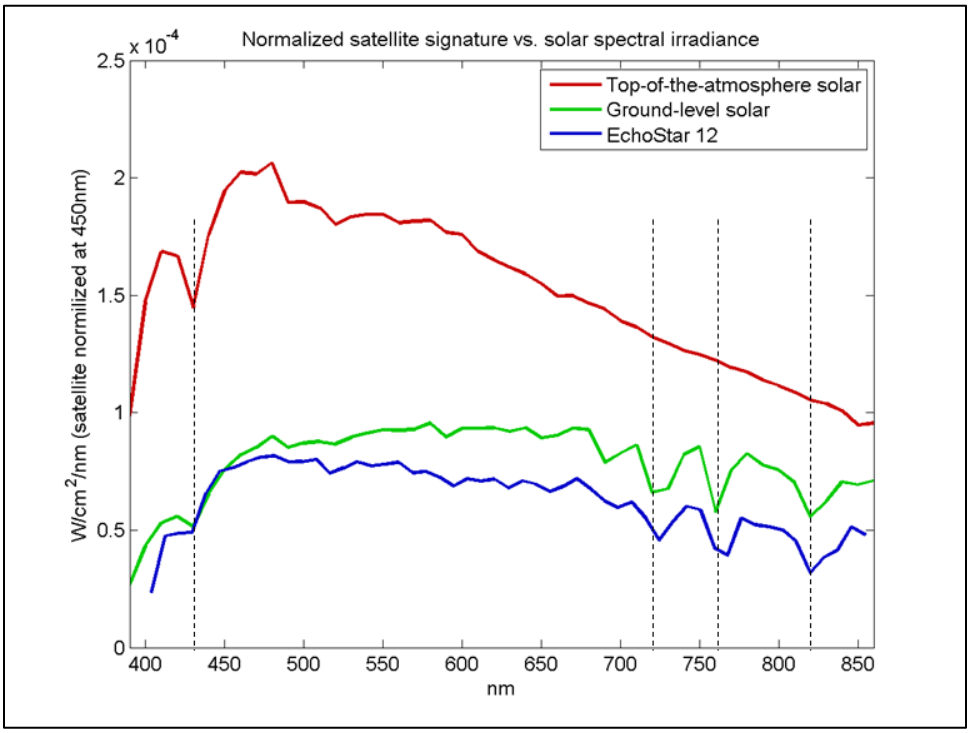

Fig. 7. Comparison of normalized EchoStar 12 spectrum with solar spectra above and below the atmosphere

6. CONCLUSIONS AND FUTURE WORK

A novel, small format proof-of-concept sensor has been developed and demonstrated for collecting spectral signatures of LEO and GEO satellites. The low cost and ease of deployment provides a new capability to use systems at different locations for simultaneous satellite signature collection. The approach of using an inexpensive, small format system with no special infrastructure requirements opens the door to more easily collecting satellite reflection measurements from multiple locations simultaneously. Using multiple systems improves the probability of data collection and provides a richer data set by having concurrent measurements at multiple reflection angles.

A primary question of this effort is whether meaningful SSA data can be produced with such a small format system. The use of the small collection aperture is the most obvious challenge, and going forward the effort will involve trading off integration time as well as spatial and spectral binning in an effort to increase signal to noise of the measured signature. Also, the optimal settings may be dependent on the object of interest; for example, LEO satellites, since they generally appear brighter than GEO satellites, would allow for shorter integration times and therefore a higher temporal sampling of the spectra, or else higher spectral resolution due to less binning required to achieve an acceptable SNR. Our working prototype system now allows us to explore these trades with a goal of determining what visual magnitude targets can be characterized.

We have shown that our system can produce useful spectral data even when solar geometry is less favorable (i.e., near equinox). This suggests that the sensitivity of system may be suitable for year-round measurements. However, at this early stage our sample size is small, and one of our future goals is to broaden our measurement set both in the number of satellites and in the number of measurements throughout the year.

7. REFERENCES

[1] K. Jorgensen, J. Africano, G. Stansbery, P. Kervin, K. Hamada, P. Sydney, "Determine the Material Type of Man-Made Orbiting Objects Using Low Resolution Reflectance Spectroscopy," *Multifrequency Electronic/Photonic Devices and Systems for Dual-Use Applications, Proceedings of SPIE Vol. 4490, pp. 237-244 (2001).*

[2] T. Schildknecht, A. Vananti, H. Krag, and C. Erd, "Reflectance Spectra of Space Debris in Geo," *Proceedings of the Advanced Maui Optical and Space Surveillance Technologies Conference*, 2009.

[3] D. Bédard, G. A. Wade, D. Monin, and R. Scott, "Spectrometric Characterization of Geostationary Satellites," *Proceedings of the 2012 AMOS Technical Conference, Kihei, Maui, HI*, 2012.

[4] R. M. Tucker, E. M. Weld, F. K. Chun, and R. D. Tippets, "Spectral Measurements of Geosynchronous Satellites During Glint Season," *Proceedings of the Advanced Maui Optical and Space Surveillance Technologies Conference, Wailea, Maui, Hawaii,* 2014.